15TH IEA HEAT PUMP CONFERENCE
MAY 26–29, 2026 | HOFBURG
VIENNA 2026
DECARBONISATION THROUGH INNOVATION

# Dynamic optimization of staged heat pump systems for the supply of high-temperature heat in industrial processes

Philipp Nguyen*, Christian Schweigler

HM Hochschule München University of Applied Sciences, Lothstr. 34, 80335 Munich, Germany

**Abstract**

Industry is a key sector for achieving the goals of the energy transition in Germany. A significant share of industry's energy requirements is accounted for by the provision of industrial process heat with process temperatures over 80 °C. The use of efficient energy converters based on renewable energy sources is crucial for decarbonizing the energy supply of industrial processes. In such applications, compression heat pumps can be used to efficiently provide the required high temperature heat.
The use of waste heat from industrial processes is a suitable source for heat pumps, for example by using the condenser output of a refrigeration cycle via the cooling water circuit. In addition to the system design, the coordination of the operating characteristics of the individual heat pumps and their interaction during operation is essential for overall efficiency. However, the dynamic optimization of staged heat pump systems based on the calculation of thermodynamic cycle processes represents a considerable computational effort. The potential for optimization is therefore rarely exploited. In this paper a method is proposed to describe staged heat pump systems using polynomials in a mixed-integer non-linear optimization problem. The use of non-linear polynomials enables the mapping of complex systems and optimization of their operation with highest energy efficiency. First, the thermodynamic cycle processes of selected heat pumps are simulated to determine the expansion and compressor efficiencies. Based on this data, the determined system characteristics can be described by a polynomial of the electrical input as a function of the required evaporator capacity and external conditions.
In the research project OpENEnD, this method is used to plan multi-stage heat pump systems for providing cooling, potable hot water, heating and process heat in a food processing plant. The aim of optimization is to improve the design of the heat pump system and its operation.



*Keywords: Operational optimization; Multi-stage heat pumps; Nonlinear programming*

## 1. Introduction

In 2024, Germany had a final energy demand of 2,249 TWh. The industry accounts for a significant portion of Germany's final energy consumption, with an energy demand of 607 TWh. This demand corresponds to around 27% of the total final energy demand [1]. The supply of process heat accounts for 67% of the energy demand of industry. However, only a limited amount of energy supply for industry is currently covered by renewable energy sources, with approximately 55% of energy demand being met directly by fossil fuels. This is especially evident in the provision of process heat, where coal and gas alone provide around 69% of energy supply [2]. In 2024, the industrial sector was the second-largest emitter, responsible for around 24% of Germany's greenhouse gas emissions [3]. Consequently, industry plays a particularly important role in achieving the greenhouse gas emission reduction targets in Germany.

To achieve the targeted reduction of emissions, a fundamental restructuring of the energy supply is necessary. The negative impact on the climate can be reduced by lowering energy demand, increasing the efficiency of energy use and switching to energy from renewable sources.

* Corresponding author. Tel.: +49 89 1265-4392
*E-mail address:* philipp.nguyen@hm.edu



*15th IEA Heat Pump Conference 2026 - HTH2.5 - https://doi.org/10.23697/70y5-w105*

The electrification of process heat supply can make a significant contribution to the decarbonization of industry. Scenarios show that by 2045, the degree of electrification in industry could rise from 30% in 2022 to 72%, replacing fossil fuels for heat supply. The use of high-temperature heat pumps to provide process heat up to 200 °C can play a crucial role in this transformation [4].

During the planning process of these energy systems, the future operation of the system components is often roughly estimated using approximate methods. Inaccuracies are due to the simplified representation of supply requirements using annual duration curves and simultaneity factors. This means that the temporal correlation between the demand patterns of individual consumers throughout the entire operating year is lost, particularly in heating and cooling supply systems.

The operating mode and efficiency of the individual units are normally described by design values without sufficient consideration of partial load conditions. Thermodynamic modeling and simulation are rarely performed for such systems due to their complexity and the associated mathematical effort. The system configuration is therefore often not optimized in terms of the selection and dimensioning of the individual components of the system and their mode of operation.

## 2. Methodology

To increase energy and cost efficiency, dynamic optimization of multi-stage heat pump systems using non-linear polynomials is proposed. The use of polynomials is intended to reduce the mathematical effort and enable in-situ optimization of combined heat pump systems under changing boundary conditions. The modeling of the heat pumps is based on a generalized modeling approach, developed for optimization of single-stage cooling supply systems [5]. This work focuses on applying this methodology for investigating the efficiency potential of multi-stage heat pump systems and the change of their operating characteristics resulting from the interconnection of several heat pumps. Fig. 1 shows the schematic process for creating and applying polynomials to optimize the energy system of a production facility.

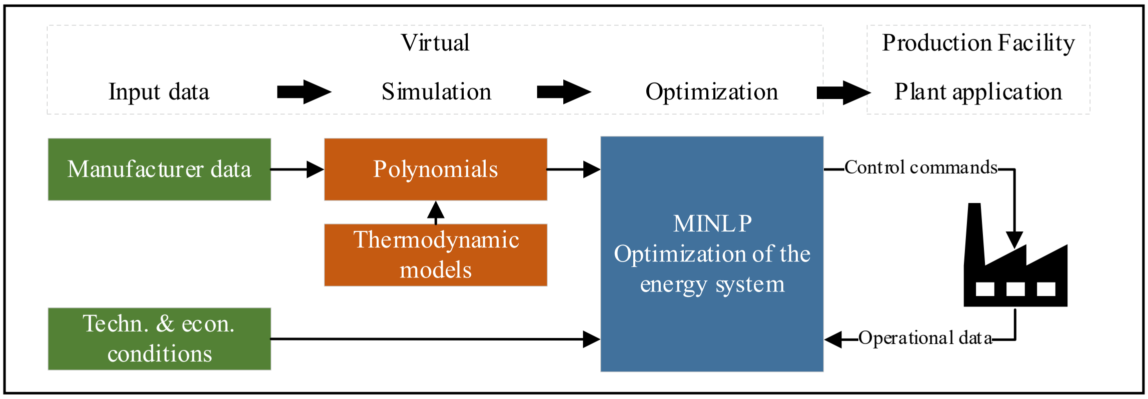


*Figure 1: Procedure for the simulation and dynamic optimization of energy systems.*

First, the input data in the form of manufacturer data and thermodynamic models of the energy system are used to create a polynomial description of the heat pumps used in the energy system. The heat pump polynomials represent the operation of the heat pumps at variable operating points. Only external parameters in the form of the current heating and cooling load, the source and sink temperatures, and the flow rates of the heat carriers passing through evaporator and condenser are used to determine the electrical power consumption of the heat pumps. The aim is to reduce the complexity of the thermodynamic models by using polynomials to enable dynamic in-situ operational optimization.

Using the heat pump polynomials and the technical and economic conditions of the application, the energy system is formulated and optimized as a mixed-integer non-linear optimization problem (MINLP). As a result of this optimization, the use of the individual heat pumps is planned and forwarded to the production environment as control commands. In return, the operating data is transferred to the optimization algorithm, which can be used to verify the current operating states of the individual heat pumps and update the heat pump polynomials if necessary.

The following section outlines the individual steps involved in creating the heat pump polynomials and their use in optimizing the operation of the energy system. First, the thermodynamic modeling of heat pumps is presented, followed by a more detailed explanation of how the heat pump polynomials are created using thermodynamic modeling and manufacturer data. Finally, the structure and specific use of the polynomials for optimizing the operation of energy systems is described.

## 3. Thermodynamic modeling of heat pumps

The first step in creating the heat pump polynomials is to model the individual components using specific thermodynamic models. Fig. 2 shows a simple heat pump system with the essential components. The internal circuit of the heat pump consists of the compressor, the throttle, the evaporator, and the condenser. Externally, pumps are used to circulate the heat carrier fluids connecting heat source and heat sink with the evaporator and condenser heat exchanger, respectively. For reasons of simplicity, other components, for example a flash tank, are not shown.

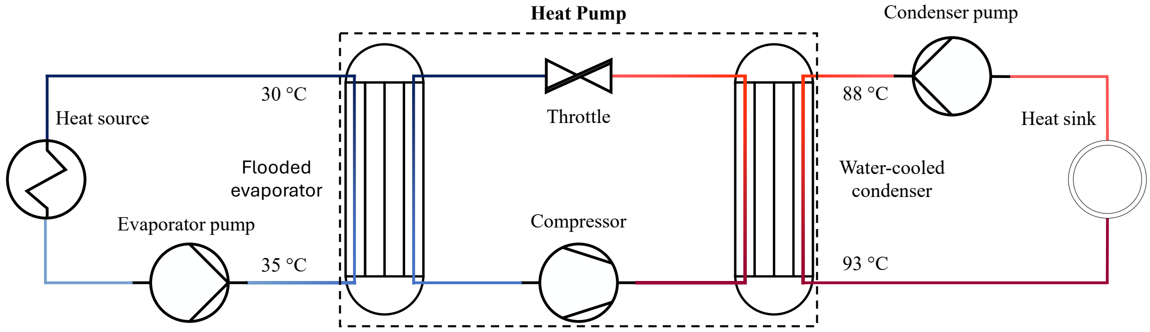


*Figure 2: Schematic representation of a simple heat pump system with example system temperatures.*

The aim of thermodynamic modeling is to create an operating map for the heat pumps under variable operating conditions. The efficiency of a real heat pump is determined on the one hand by the temperature differences at the heat exchangers (internal/external) and on the other hand by the internal losses in the heat pump circuit. Fig. 3 shows an example of a heat pump cycle in a log(p)-h diagram with the entropically averaged temperatures $T_i$ (internal) and $t_i$ (external). Losses occur during the compression of the refrigerant (enthalpy difference between state points 2 and $2_{id}$) and the isenthalpic expansion at the throttle (enthalpy difference between state points 4 and $4_{id}$). Both changes of state deviate from the ideal isentropic cycle.

The Coefficient of Performance (COP) for heat pumps and the Energy Efficiency Ratio (EER) for chillers describe the efficiency of the current operation as a performance factor and, in reversible operation, depend exclusively on the external temperatures of the heat source ($t_0$) and the heat sink ($t_1$) as $COP_{rev}$ and $EER_{rev}$. Assuming reversible operation, the temperature differences between the respective heat transfer media in the heat exchangers are negligible, and the internal thermodynamic cycle of the heat pump operates completely loss-free. In reality, however, driving temperature differences between the external heat carriers ($t_1$ and $t_0$) and the internal processes ($T_0$ and $T_1$) are required for the heat transfer at the evaporator and condenser, respectively. Consequently, the reversible performance factors are reduced to the endoreversible $COP_{endo}$ and $EER_{endo}$.

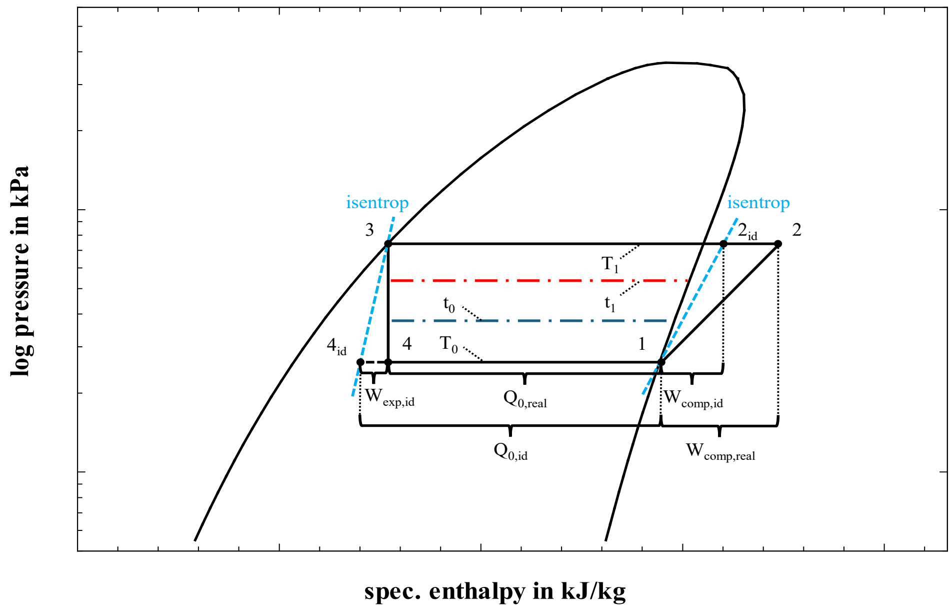


*Figure 3:Heat pump cycle in log(p)-h diagram with entropically averaged temperatures (internal/external).*

The $EER_{endo}$ can be calculated using the ratio of the useful evaporator energy $Q_{0,id}$ and the net demand of mechanical work, given by the difference between the isentropic compressor work $W_{comp,id}$ and the work obtained during isentropic throttling $W_{exp,id}$. In relation to the ideal condenser output $Q_{1,id}$, the equation is reduced to the difference of the $COP_{endo}$ and the factor 1. By definition, the heat pump $COP_{endo}$ and the chiller $EER_{endo}$ differ by 1, as can be deduced from the overall balance of heat input $Q_{0,id}$, heat output $Q_{1,id}$ and net mechanical work as difference between $W_{comp,id}$ and $W_{exp,id}$.

$$EER_{endo} = \frac{T_0}{T_1 - T_0} = \frac{Q_{0,id}}{W_{comp,id} - W_{exp,id}} = COP_{endo} - 1 \tag{1}$$

The irreversibilities in the internal cycle during compression and expansion of the refrigerant, expressed by the compressor efficiency $\eta_{comp}$ and the expansion efficiency $\eta_{exp}$, reduce the efficiency of the endoreversible cycle. $EER_{real}$ is calculated as the ratio of the amount of cold delivered $Q_{0,real}$ and the difference between the compressor work $W_{comp,real}$ and the enthalpy gain of the expansion $W_{exp,real}$. In practical applications, isenthalpic throttling is applied and the potential enthalpy gain provided by an isentropic expansion is usually not utilized, which simplifies the calculation of the $EER_{real}$ accordingly.

$$EER_{real} = \frac{Q_{0,real}}{W_{comp,real}} = COP_{real} - 1 \tag{2}$$

According to [5] the ratio of the performance factors $EER_{endo}$ to $EER_{real}$ is described by the cycle quality $\eta_{endo}$, which takes into account losses during refrigerant compression and isenthalpic expansion. The loss mechanisms can be separated by formulating the efficiency of compression and expansion.

$$\eta_{endo} = \frac{EER_{real}}{EER_{endo}} = \frac{W_{comp,id}}{W_{comp,real}} \cdot \left(1 - \frac{W_{exp,id}}{W_{comp,id}}\right) \cdot \left(1 - \frac{W_{exp,id}}{Q_{0,id}}\right) = \eta_{comp} \cdot \eta_{exp} \tag{3}$$

In conventional heat pumps, with isenthalpic expansion, the efficiency of expansion solely depends on the properties of the refrigerant and the pressure ratio of the internal thermodynamic cycle. Based on this approach, the specific efficiency of the heat pump $COP_{real}$ is governed by the characteristics of the compressor efficiency $\eta_{comp}$, the expansion efficiency $\eta_{exp}$ and the $EER_{endo}$.

$$COP_{real} = EER_{real} + 1 = \eta_{comp} \cdot \eta_{exp} \cdot EER_{endo} + 1 \tag{4}$$

Herein, $EER_{endo}$ of the internal cycle reveals the drop of efficiency relative to the theoretical optimum, given by the temperature levels of the external heat carriers. Summarizing all irreversibilities, the overall quality of the thermodynamic cycle is obtained.

$$EER_{real} = \eta_{total} \cdot EER_{rev} \tag{5}$$

The following section examines the loss mechanisms during compression and expansion in terms of compressor efficiency and expansion efficiency, as well as heat transfer. The results can be used to create polynomials for simplified description of the operating characteristics of heat pumps. For this purpose, a chiller with a scroll compressor (refrigerant R290) with a supply temperature of 6 °C and a high-temperature heat pump with a piston compressor (refrigerant R1234ze(E)) with a supply temperature of 93 °C are examined.

### *3.1. Compressor efficiency*

The compressor is one of the main components of the heat pump. It takes in the refrigerant leaving the evaporator and compresses it to a higher-pressure level. There are different types of compressors, the most common being piston compressors, screw compressors, scroll compressors, and turbo compressors. These differ in terms of their design, areas of application, and efficiency.

Cubic compressor polynomials can be used to describe the operating characteristics of such compressors according to DIN EN 12900. These polynomials enable the electrical power consumption, cooling capacity, current, and mass flow rate to be calculated for a given refrigerant, depending on the evaporator temperature $T_0$, the condensation temperature $T_1$, and the operating frequency, i.e. the speed of rotation of the electric drive of the compressor.

Open-access software provided by manufacturers can be used to examine various compressor types using these compressor polynomials. For the purposes of this study, compressor type GSP80485ZL for the refrigeration machine with scroll compressor was selected and compressor type 6FEH-50Y for the heat pump with piston compressor [6]. Compressor efficiency can be calculated using a cycle calculation based on the compressor polynomials as the ratio of isentropic to actual compressor work. Fig. 4 shows the compressor maps of the selected compressors with variations in evaporation and condensation temperature as well as the operating frequency.

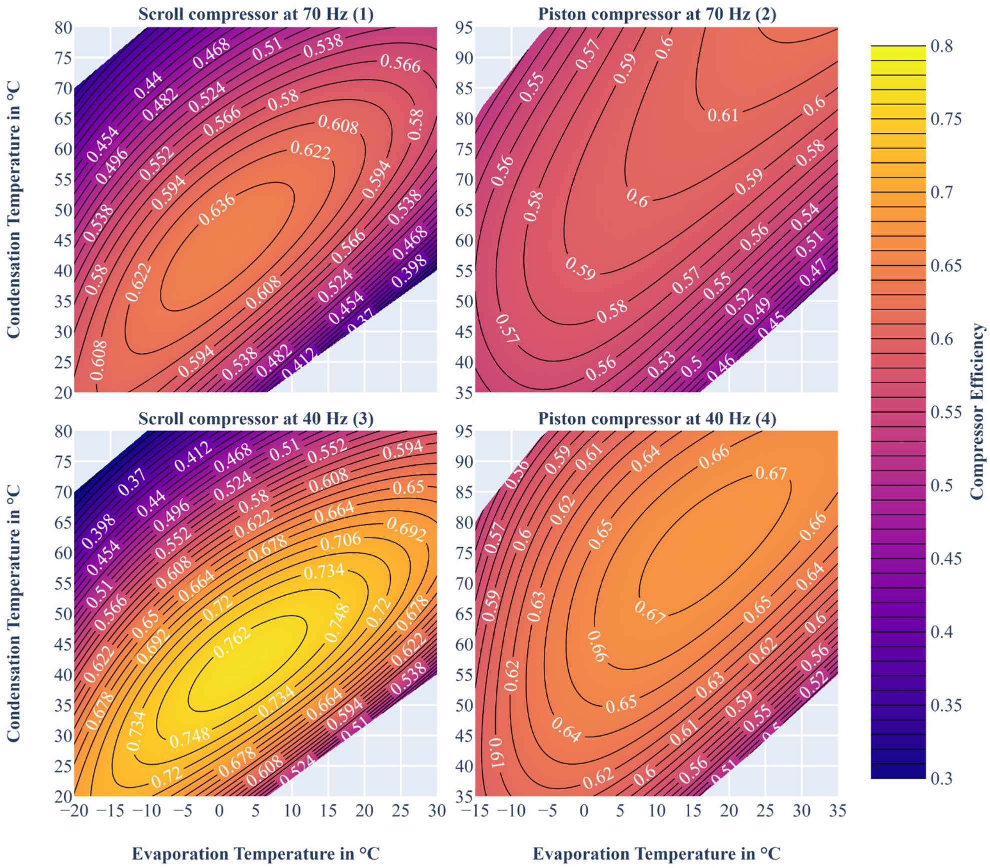


*Figure 4: Compressor map of a frequency-controlled scroll compressor (1 & 3) and piston compressor (2 & 4) at frequencies of 40 Hz and 70 Hz with a variation in evaporation and condensation temperature.*

The efficiency of the scroll compressor varies greatly depending on the temperature lift from evaporation to condensation and the operating frequency from around 30 to 80%. In comparison, the piston compressor has a more stable compressor efficiency of 50 to 60% across a wide operating range. However, the computational effort required to consider different operating states is high, as the compressor polynomials only apply to distinct operating frequencies. This means that the coefficients for the individual operating states must either be determined individually or the load of the compressor depending on the speed of rotation must be integrated into the mathematical regression as an additional degree of freedom. Consequently, for the calculation of the $COP_{real}$ during operation of the heat pump with variable load, the compressor efficiency is parameterized based on the evaporation and condensation temperatures and the part load factor (PLF). The part load factor refers to the current evaporator capacity in relation to the nominal evaporator capacity [5].

$$PLF = \frac{\dot{Q}_0}{\dot{Q}_{0,design}} \tag{6}$$

Simplifying the cubic compressor polynomial to a quadratic function reduces the mathematical effort and enables a simple representation of the partial load behavior of the compressors. Finally, the compressor efficiency is described using a second-degree polynomial depending on the evaporation and condensation temperature as well as the PLF [5].

$$\eta_{comp} = c_0 + c_1 \cdot T_0 + c_2 \cdot T_1 + c_3 \cdot PLF + c_4 \cdot T_0^2 + c_5 \cdot T_1^2 + c_6 \cdot PLF^2 \tag{7}$$

*3.2. Expansion efficiency*

Expansion efficiency describes the effect of isenthalpic throttling. Figure 5 shows this efficiency for R290 and R1234ze(E) across the operating range analyzed.

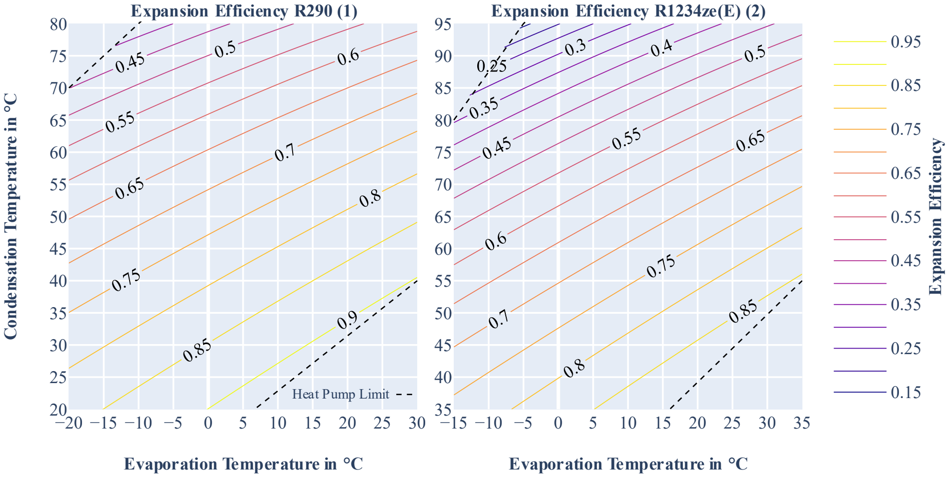


*Figure 5: Expansion efficiency for refrigerants R290 (1) and R1234ze(E) (2) with a variation in evaporation and condensation temperature within the operating limits of the compressor types examined.*

It can be seen here that the expansion efficiency decreases significantly as the temperature difference increases. In the operating range examined, the expansion efficiency for refrigerant R290 varies between around 40% and over 90%, and for refrigerant R1234ze(E) between around 20% and 85%. To determine the expansion efficiency without an exact thermodynamic cycle calculation, it can be expressed using a quadratic polynomial as a function of the evaporation and condensation temperatures [5].

$$\eta_{exp} = c_0 + c_1 \cdot T_0 + c_2 \cdot T_0^2 + c_3 \cdot T_1 + c_4 \cdot T_1^2 \tag{8}$$

*3.3. Heat exchange at heat source and heat sink*

For accurate modeling of heat transfer at the evaporator and condenser, sectional modeling of the heat exchanger is necessary. Depending on the aggregate state, the fluid properties of the refrigerant and the operating characteristics of the heat exchanger are used to calculate heat transfer as accurately as possible. However, such a detailed calculation is unsuitable for in-situ optimization. Consequently, a simplified model of heat transfer according to [5] is used. For this purpose, the part flow factor (PFF) is introduced, which represents the ratio of the external volume flow $\dot{V}$ to the nominal external volume flow $\dot{V}_{nom}$. This is calculated for both the evaporator and the condenser.

$$PFF = \frac{\dot{V}}{\dot{V}_{nom}} \tag{9}$$

To obtain a simplified characterization of the heat transfer, the closest approach temperature difference $\Delta t$ between the internal process and the external heat carrier is used. This characteristic temperature gradient $\Delta t$ occurs at the outlet of the heat exchanger, i.e., as the difference between the source outlet temperature and evaporation as well as between condensation and sink outlet temperature. With knowledge of the design temperature gradient $\Delta t_{nom}$, a simplified calculation based exclusively on manufacturer data is possible [5].

$$\Delta t = \Delta t_{nom} \cdot PFF \cdot PLF \tag{10}$$

*3.4. Polynomial models for the characterization of heat pumps*

Using the modeling work, a $COP_{ETM}$ or $EER_{ETM}$ can be determined with the aid of a cubic polynomial to calculate the electrical power consumption as a function of the evaporator capacity, the external source and sink temperatures, and the external volume flows. To do this, compressor polynomials are first used to establish an operating map with internal process temperatures ($COP_{Cycle}$), which is then used to calculate a $COP_{ITM}$ according to Eq. (4).

Using the heat transfer model, an operating map can be established by using $\eta_{comp}$ and $\eta_{exp}$ to enable parameterization of electrical power consumption based on external conditions for creating the cubic polynomial function for calculation of $COP_{ETM}$.

Fig. 6 shows the simulated operating characteristics $COP_{ITM}$, $COP_{ETM}$, starting from $COP_{Cycle}$, and the evaluation metrics of the fit functions using the variance $R^2$ and the root mean squared error RMSE. With an $R^2$-score of over 0.99 and RMSE deviations between 0.01 and 0.05, a sufficiently good approximation of the detailed cycle calculation ($COP_{Cycle}$) to the simplified modeling calculation ($COP_{ETM}$) is achieved.

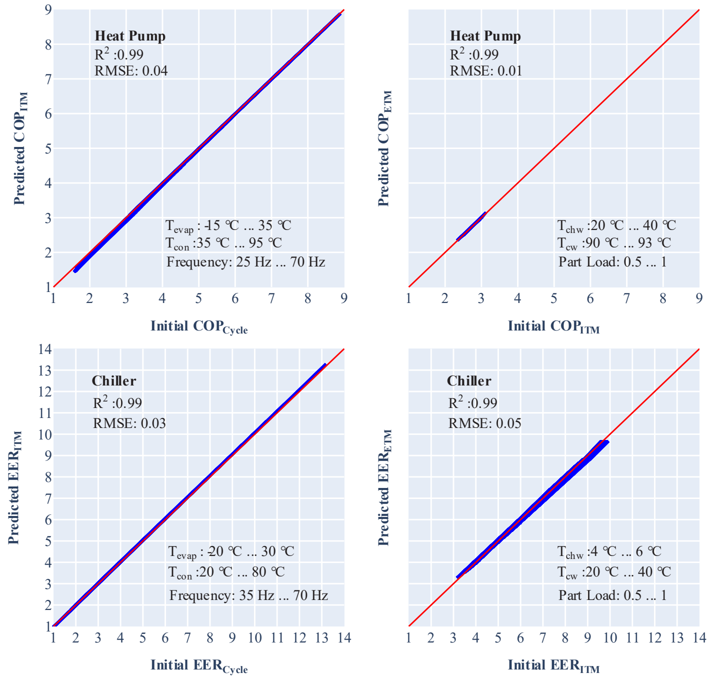


*Figure 6: Quality of simulated operating maps using polynomials based on variation $R^2$ and root mean squared error RMSE within the limits of operation of the heat pump and chiller.*

### 3.5. Operating characteristics of multi-stage heat pump systems

To illustrate the changing operating characteristics resulting from the interconnection of different heat pumps, the coupled operation of a chiller and a heat pump circuit is analyzed; for system details, see Fig. 7.

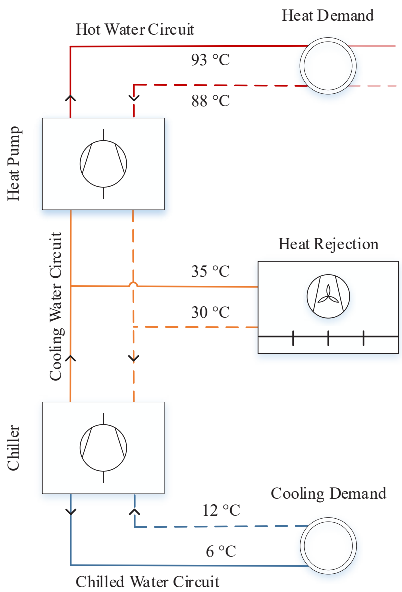


*Figure 7: Exemplary heat pump system with a high-temperature heat pump and a chiller coupled via a common cooling water circuit.*

The chiller is designed to cover chilled water demand at a flow temperature of 6 °C, with the resulting waste heat being transferred to a cooling water network. This heat can now be dissipated into the environment using a heat rejection system or used as a source for the heat pump. The heat pump is designed to deliver a hot water flow temperature of 93 °C. Alternatively, the heat demand can be met by additional heat sources.

Fig. 8 shows the $COP_{real}$ and $EER_{real}$ curves for the heat pump and chiller at varying upper cooling water temperatures and load conditions, as well as the system $COP_{real}$, defined as the relation of the total cooling and heating capacity and the total electrical power demand.

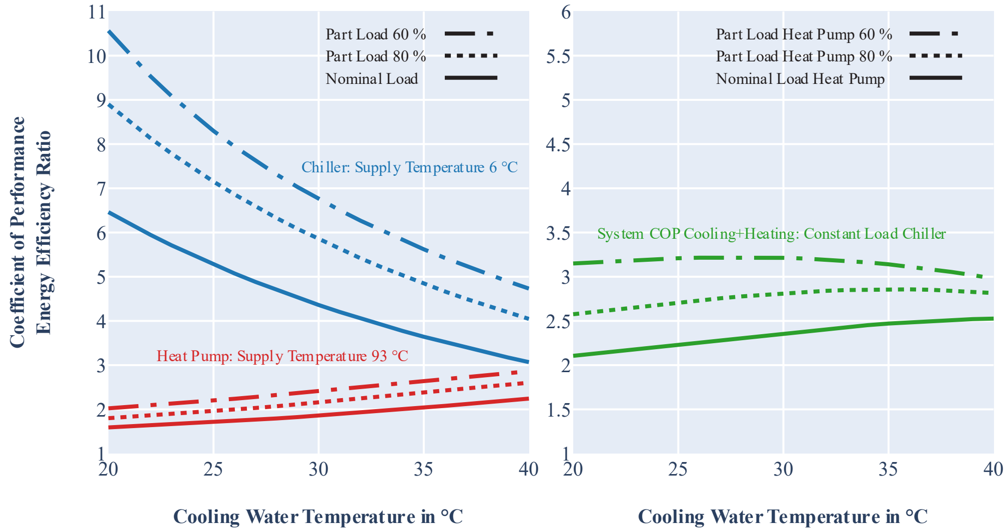


*Figure 8: Comparison of the $COP_{real}$ and $EER_{real}$ of the heat pump and the chiller with variations in the upper cooling water temperature and load conditions, as well as the system $COP_{real}$ (cooling & heating) at constant cooling capacity.*

The optimal values for the $COP_{real}$ for the heat pump for the specified load conditions are found for operation with lowest temperature lift from heat source to heat sink, i.e., at a cooling water temperature of 40 °C. The same applies to the chiller at a cooling water temperature of 20 °C. When considering the system $COP_{real}$, there is an optimal cooling water temperature depending on the load condition of the two system components. The strongest influence of the temperature level of the cooling water can be observed under the heat pump's nominal load conditions. Here, the $COP_{real}$ varies from 2.11 at a cooling water temperature of 20 °C to 2.53 at 40 °C (corresponding to a relative improvement of roughly 20%). Fig. 9 shows the optimal cooling water temperature with the corresponding system $COP_{real}$ for a variation of the individual load states of the heat pump and the chiller. Lower cooling water temperatures are especially advantageous when the heat pump output is low.

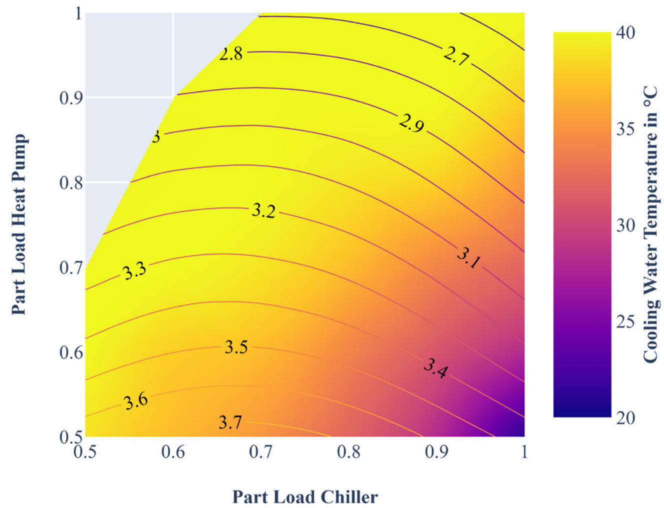


*Figure 9: Optimal cooling water temperature and respective system $COP_{real}$ at variable load of chiller and heat pump.*

As the proportion of heat pump capacity relative to cooling capacity increases, the optimal cooling water temperature increases from 21 °C to 40 °C. Particularly when considering the refrigeration machine under partial load conditions with a simultaneous increase of the load of heat pump, higher cooling water temperatures become advantageous in terms of the system $COP_{real}$.

The system $COP_{real}$ varies across the entire operating range examined between 2.53 at full load of the chiller and the heat pump with an optimal cooling water temperature of 40 °C and a system $COP_{real}$ of 3.74 at 70% partial load of the chiller and 50% partial load of the heat pump at a temperature of 35 °C.

The investigation of the operating characteristics of the heat pump and the chiller has shown that there are significant differences in the efficiency of the overall system in real operation due to the type of compressor used and the choice of refrigerant. These become particularly apparent under variable load conditions, i.e. source and sink temperature, as well as heating and cooling load. This demonstrates that dynamic optimization of heat pump operation has the potential to make cooling and heating supply more efficient and cost-effective on a demand-oriented basis.

## 4. Optimization of the energy system in a food production facility

The proposed modeling for heat pumps can be used to optimize more complex energy systems. Here, the energy system of a food factory, which requires hot water up to 93 °C and cooling down to a brine temperature of -14 °C, will be examined as an example. The system represents the planning case of a real application and is shown in Fig. 10.

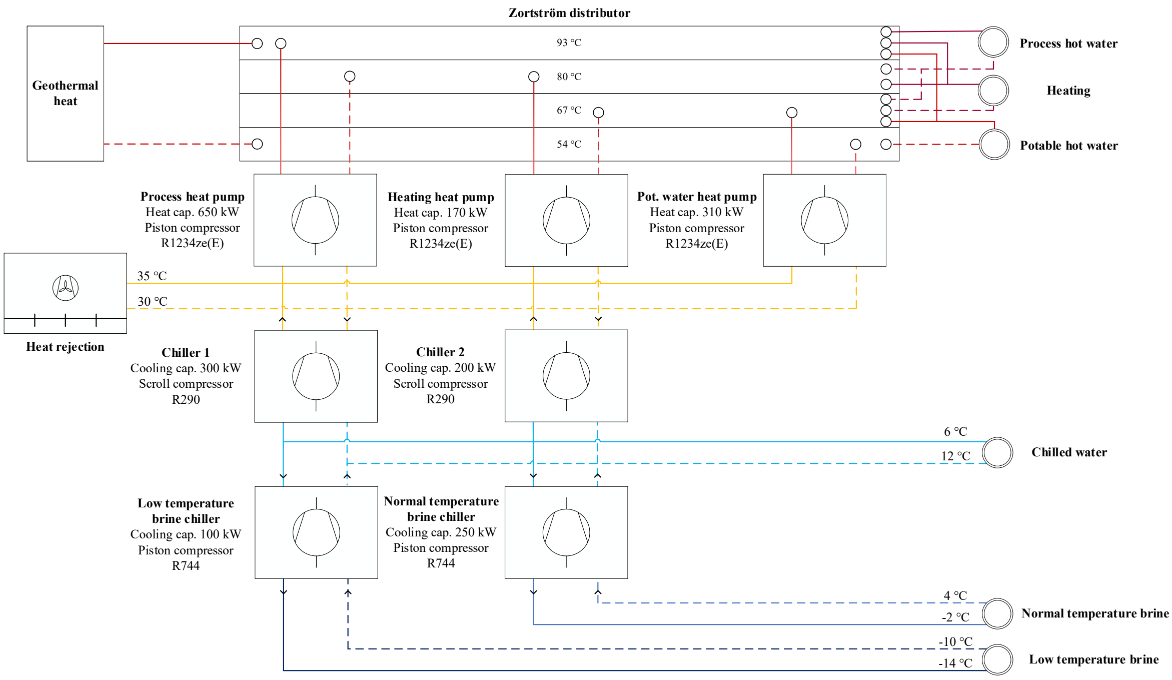


*Figure 10: Energy system for supplying the facility with heating and cooling regarding different supply temperatures.*

There are three temperature levels for heat demand ranging from 67 °C to 93 °C, as well as three temperature levels for cooling demand ranging from 6 °C chilled water to -14 °C brine. Normal and low-temperature cooling is to be provided by two subcritical $CO_2$-systems. The resulting waste heat and the cooling load of the chilled water system is discharged to a cooling water network by means of two chillers.

In the next step, the waste heat can either be released to the environment via heat rejection or raised to a higher temperature level by three separate heat pumps. In addition to the heat pumps, the heat demand can also be provided by a connected geothermal district heating network. The temperature levels for heat generation and heat supply to the consumers are connected to each other using a Zortström distributor.

Fig. 11 shows the operating data for heating and cooling demand for one work week of operation. Looking at the individual curves, heating demand exceeds cooling demand. There is a high but strongly fluctuating demand for process heat. The demand for potable hot water and heating plays a minor role.

A more detailed examination of cooling demand shows that, in contrast to heating demand, there are cyclical cooling capacity needs. In terms of peak capacity, the three cooling demands are comparable, with the normal cooling demand still dominating. It is evident that the constant demand for cooling and heating provides good opportunities for heat recovery and upgrading of the waste heat for heating purposes.

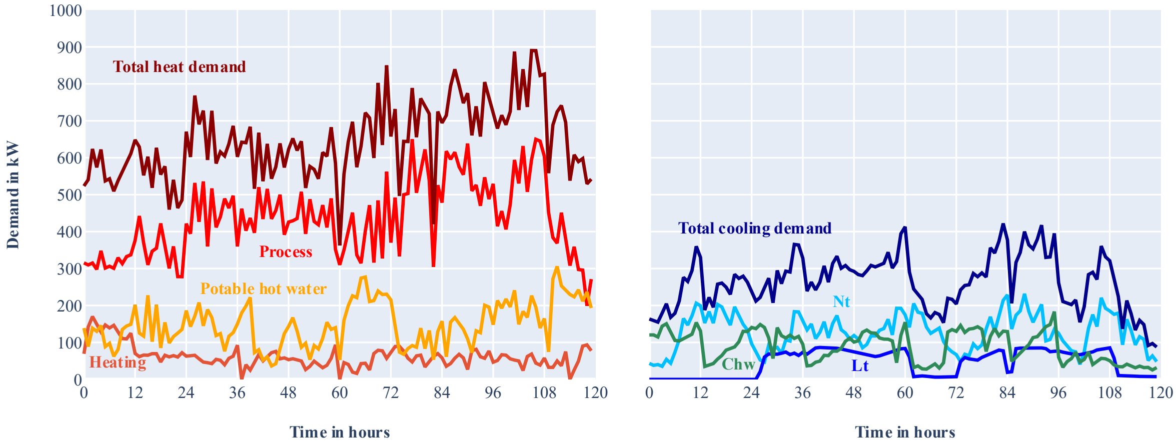


*Figure 11: Operating data for heat demand (process heat, potable water, heating) and cooling demand (normal temperature (Nt), low temperature (Lt), chilled water (Chw)) for one working week in hourly resolution.*

For dynamic optimization of the energy system, the operating characteristics of the heat pumps and chiller are modeled using polynomials according to the methodology presented in Chapter 3 and used in a MINLP system model. The optimization problem is implemented in Python using the Pyomo library. The Baron Solver is applied to solve the optimization problem.

To illustrate how the optimization tool works, two scenarios are examined: one with a static setpoint for the cooling water flow temperature of 20 °C and the other with dynamic optimization of the cooling water temperature between 20 °C and 40 °C. A price of 17.8 ct/kWh has been assumed for grid electricity [7] and electricity production costs of 5.0 ct/kWh have been assumed for PV electricity. The geothermal district heating price is 16.2 ct/kWh. Optimization is performed at hourly intervals.

### *4.1. Formulation of the optimization problem*

In this example, the energy system is optimized by minimizing total costs over the period under analysis. The costs are calculated by multiplying the respective prices by the demand for PV electricity $P_{pv,dem}$, grid electricity $P_{grid,dem,}$ and district heating $\dot{Q}_{dh,dem}$.

$$min \sum_{t=1}^{T} cost_t = price_{pv} \cdot P_{pv,dem,t} + price_{grid} \cdot P_{grid,dem,t} + price_{dh} \cdot \dot{Q}_{dh,dem,t} \tag{11}$$

The electrical energy demand of the system components $P_{el}$ must be covered by $P_{pv,dem}$ and $P_{grid,dem}$.

$$P_{el,t} = P_{pv,dem,t} + P_{grid,dem,t} \tag{12}$$

The electrical energy requirement is calculated from the sum of the consumers (chiller $P_{el,ch}$, heat pump $P_{el,hp}$, pumps $P_{el,pu}$, and heat rejection $P_{el,ct}$) and the multiplication of the respective binary decision variables x.

$$P_{el,t} = x_{i,t} \cdot P_{el,ch,i,t} + x_{j,t} \cdot P_{el,hp,j,t} + x_{k,t} \cdot P_{el,pu,k,t} + x_{l,t} \cdot P_{el,ct,l,t} \tag{13}$$

The electrical power consumption of the pumps $P_{el,pu}$ is a second-degree polynomial depending on the volume flow, one is installed at each supply flow of the producers and consumers. The electrical power consumption of the heat rejection $P_{el,ct}$ is a third-degree polynomial depending on the transferred waste heat, the temperature difference between the ambient air temperature and the cooling water return temperature, and the cooling water volume flow. The sum of $P_{el,pu}$ und $P_{el,ct}$ is referred to below as auxiliary power.

The cooling demand $\dot{Q}_{c,dem}$ is continuously covered by the cooling capacity of the chiller $\dot{Q}_{ch}$.

$$\dot{Q}_{c,dem,i,t} = \dot{Q}_{ch,i,t} \tag{14}$$

Simultaneously, the heat demand $\dot{Q}_{h,dem}$ must be met, either through district heating $\dot{Q}_{dh,dem}$ or the heat output of the heat pumps $\dot{Q}_{hp}$.

$$\dot{Q}_{h,dem,j,t} = \dot{Q}_{dh,dem,j,t} + \dot{Q}_{hp,j,t} \tag{15}$$

### 4.2. Optimization results

The simulation results for the optimized energy supply of the food factory are shown in Fig. 12. The decisive variable for the optimal operation of the integrated heating and cooling system is the temperature of the cooling water link between the chillers and the heat pumps. Resulting from the simultaneity of heating and cooling demand, the optimum setting of the cooling water temperature predominantly stays close to the maximum limit at 40 °C. The total electrical energy requirement is almost identical in both scenarios, with a shift in the electrical energy demand from the heat pumps to the chillers in the optimized scenario.

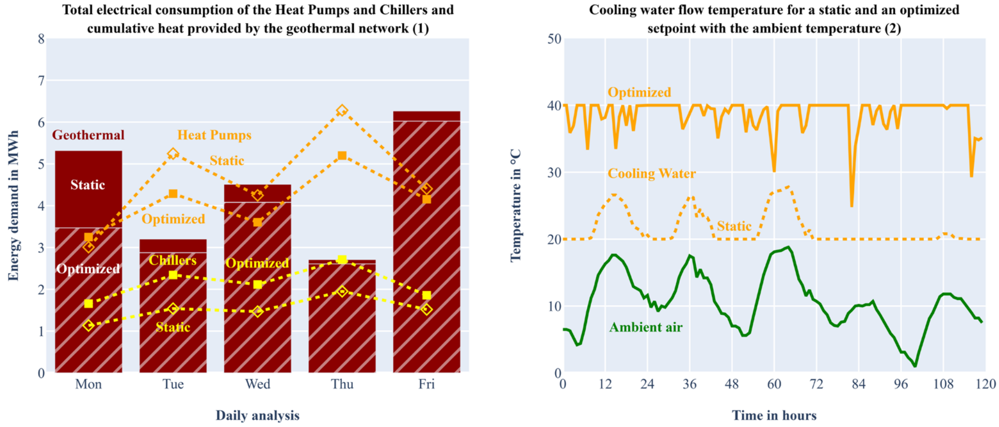


*Figure 12: Comparison of the cumulative energy demand for supplying the food factory with heating and cooling (1) resulting from optimization of the cooling water flow temperature versus a static setting (2).*

The increased cooling water temperature during optimized operation result in a reduction of the district heating demand by around 2.96 MWh compared to the static setting of the cooling water temperature. To classify the optimization results, Fig. 13 shows the cooling and heating capacities supplied, the electrical power consumption, the performance factors, and the costs. For the same cooling and heating requirements, the system $COP_{real}$ are almost identical (improvement from 2.78 to 2.86), but the costs have been reduced by almost 10% from 6,417 Euro to 5,816 Euro. This is due to the significantly lower demand for district heating.

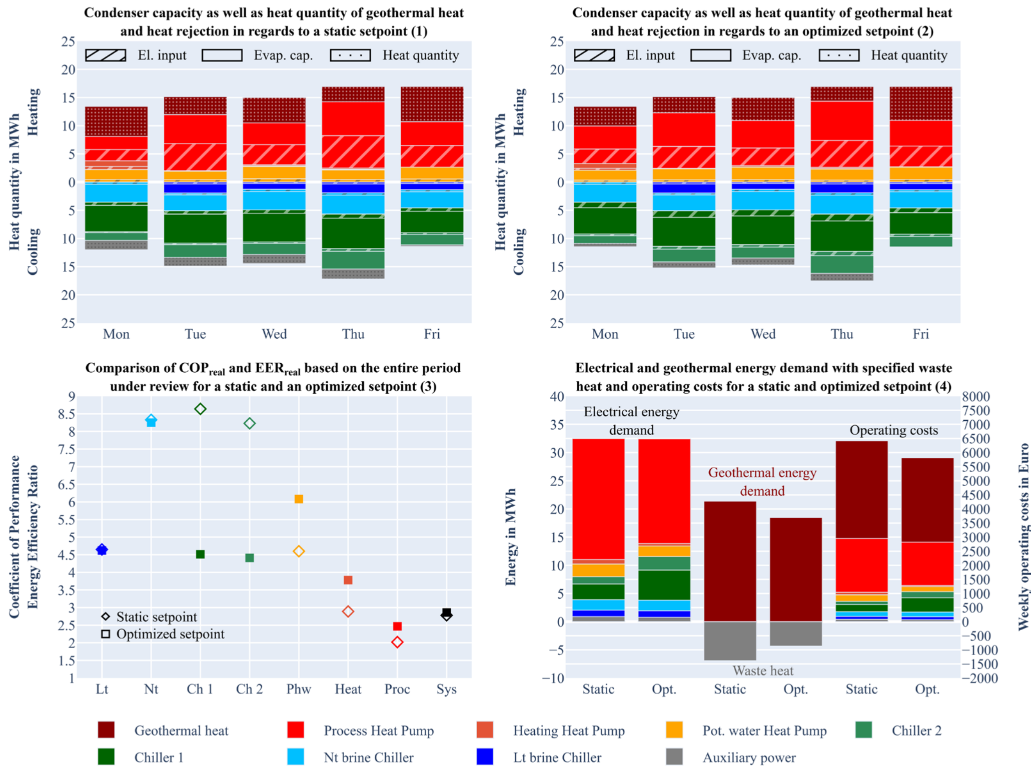


*Figure 13: Comparison of the heat quantities of the heat and cold generators (1 & 2), the $COP_{real}$ and $EER_{real}$ (3) and the cumulative energy demand and operating costs (4) for a static or optimized setting of the cooling water link between chillers and heat pumps.*

Due to the higher cooling water temperature and the corresponding larger temperature lift, the $EER_{real}$ of chiller 1 and 2 decreases significantly from 8.64 to 4.51 and from 8.23 to 4.41, respectively. This increases the amount of waste heat available in the cooling water network, which serves as heat source for the heat pumps. In addition, the temperature lift of the heat pumps decreases, which is reflected in an improved $COP_{real}$. Given the same load situation for the heat pumps, the increase of the cooling water temperature level and the associated change of the EER and COP values result in both a larger output of waste heat of the cooling system, and a larger source capacity utilized by the heat pumps. The cost-intensive supply of heat through the geothermal district network can thus be reduced in the application case.

## 5. Conclusion

This paper aims for the dynamic optimization of multi-stage heat pump systems for the provision of high-temperature heat using simplified polynomials to map the operating characteristics. First, operating maps were created using cycle calculations with the compressor and expansion efficiency. It was found that the choice of compressor type and specific refrigerant has a significant impact on the efficiency of the system. Using a simplified heat exchanger model, a cubic polynomial was created from this data to calculate the electrical power consumption of the heat pump as a function of the required cooling capacity, external temperatures, and volume flows. The evaluation metrics $R^2$ and RMSE confirmed a sufficiently good approximation to the complex cycle calculation, with an $R^2$-score of over 0.99 and RMSE between 0.01 and 0.05 for the calculated $COP_{real}$. The operating characteristics of combined heat pump systems were investigated using the polynomials created. It was shown that, by exploiting the characteristics of the heat pumps and chillers, it is possible to increase the system $COP_{real}$. Based on the total cooling and heating output, $COP_{real}$ increased by 20% by adjusting the intermediate temperature level. In the case study of energy supply for a food factory, the use of the optimization model in a multi-stage cooling and heating supply system was investigated. Cost optimization was carried out regarding electricity and district heating demand. The results show that a cost reduction of around 10% can be achieved through reduced district heating demand accomplished by improved heat recovery compared to a static setpoint for the temperature of the linking cooling water system.

In summary, dynamic optimization of multi-stage heat pump systems can increase overall energy efficiency and reduce costs. The realistic representation of the operating characteristics of individual heat pumps can be further enhanced during operation by adjusting the polynomial component models.

## Acknowledgements

The research project OpENEnD is funded within the framework of the BayVFP Digitalisierung by the Bavarian Ministry of Economic Affairs, Regional Development and Energy with the funding code DIK0417. We would like to express our gratitude to our project partners Sustainable Exergy and Trane Roggenkamp for their valuable insight and constructive cooperation.

## References

[1] AG Energiebilanzen e.V, Auswertungstabellen zur Energiebilanz in Deutschland: Daten für die Jahre von 1990 bis 2024, Berlin, 2025

[2] AG Energiebilanzen e.V, Anwendungsbilanzen zur Energiebilanz in Deutschland: Endenergieverbrauch nach Energieträgern und Anwendungszwecken, Berlin, 2025

[3] Expertenrat für Klimafragen, Prüfbericht zur Berechnung der deutschen Treibhausgasemissionen für das Jahr 2024 und zu den Projektionsdaten, p. 65, Berlin, 2025

[4] Thelen, C., Nolte, H., Kaiser, M., Jürgens, P., Müller, P., Senkpiel, C., Kost, C., Wege zu einem klimaneutralen Energiesystem: Bundesländer im Transformationsprozess, p. 62, Fraunhofer ISE, Freiburg, 2024

[5] Bentz, J., Schweigler, C., Klüglich, J., Roggenkamp, T., Dynamische Optimierung von Kälteversorgungssystemen, München, 2024

[6] BITZER Kühlmaschinenbau GmbH, Bitzer Software, https://www.bitzer.de/websoftware/, Sindelfingen, accessed on 17.11.2025

[7] BDEW Bundesverband der Energie- und Wasserwirtschaft e. V., BDEW-Strompreisanalyse Oktober 2025, Berlin, 2025